

Deep UV Laser Induced Native Fluorescence and Resonance Raman Detectors for Capillary Electrophoresis March 15, 2004

Overview

DNA sequencing is the gold standard for identification of genetic material. And capillary electrophoresis provides the greatest speed, accuracy and ease in automation of any of the DNA sequencing instrumental methods. Capillary electrophoresis (CE) is a separation technology. CE can cleanly separate trace samples as small as 1pL(10^{-12} L), whether they are ions, small molecules, or large biomolecules. Detection sensitivity has been the primary system limitation for this technology. However, using deep UV laser induced native fluorescence detectors, detection limits are approaching zeptomole (10^{-21} mole) level. A major factor that has limited the broad acceptance and utility of this technology has been the lack of a suitable deep UV laser. A suitable deep UV laser is one that emits a few mW in deep UV wavelengths matching the electronic absorption bands of the analytes of interest, yet is compact, air cooled, requires low input power, and is inexpensive. For most biomolecules ideal laser wavelengths are in the 220nm to 290nm range. Without such a laser it is necessary to derivatize the analyte by tagging with any of several dyes which absorb at visible wavelengths and allow the use of a visible laser¹. Derivatization of an analyte limits the types of molecules that can be studied and can lower the overall CE detection sensitivity. In addition, derivatization also reduces CE's ability to find unexpected analytes in complex systems and can perturb the chemistry being studied.

The use of laser induced native fluorescence (LINF) detection in CE has been studied by several researchers^{2,3,4}. Below is a figure illustrating the separation of a mixture of 2.5×10^{-4} M tryptophan and 5×10^{-3} M phenylalanine using a wavelength resolved native fluorescence detector with excitation at 244nm using a water-cooled, frequency doubled, argon ion laser drawing about 15kW of power.

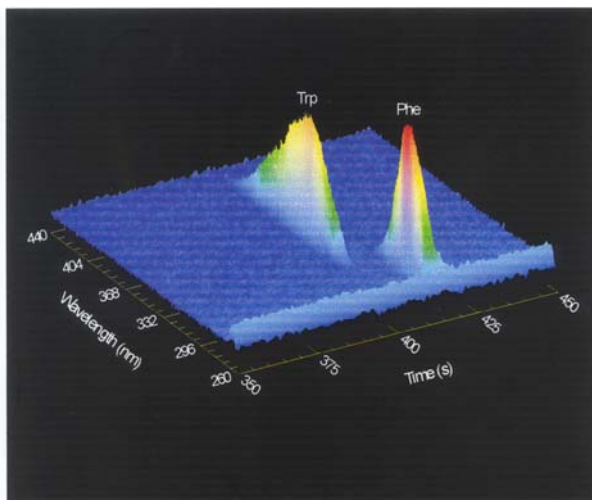


Figure 1. CE electropherogram with 244nm laser induced native fluorescence detector (Courtesy of Prof. J.V. Sweedler, U. Illinois/Champaign/Urbana)

¹ Glazer, A.N., K.Peck, and R.A. Mathies, Proc.Natl.Acad.Sci.,USA, 87, 3851-3855,(1990).

² S.Nie, R. Dadoo, and R.N.Zare, Anal.Chem.65,3571-3575, 1993

³ T.T.Lee, and E.S. Yeung, Anal. Chem, 64, 3045-3051, 1992

⁴ Zhang, X and J.V. Sweedler, Anal. Chem, Nov. 2001.

Advantages of Photon Systems' Deep UV Lasers

Photon Systems is developing a family of deep UV lasers that we believe will be the enabling technology for the commercial use of LINF in CE and HPLC. The principle advantages of our lasers for CE/LC/LINF include:

- An array of deep UV emission wavelengths at 224nm, 248nm, 260nm and 272nm compatible with optimum excitation of native fluorophors and high levels of discrimination against background materials.
- High quasi-cw output power, 20mW to 50mW at 224nm or 40mW to 200mW at 248nm with pulse widths from 10's to 100's of microseconds.
- Very inexpensive (<\$5000) , less than 10% of the cost of other deep UV lasers. OEM costs can be less than \$3000.
- Very low power consumption (<10W), can be powered from the USB port of typical computers.
- "Soft" output pulse compared to 266nm DPSS lasers, thereby minimizing photochemical and thermal damage of analyte.
- Small size: 2"x5"x14" for complete laser system including laser tube, power supply and control electronics. In other configurations the laser tube and power supply can be separated to make a smaller laser head of 12" long by 1.5" diameter.

Laser induced fluorescence detection systems currently employed in CE systems such as the Beckman P/ACE MDQ employ a CW laser with a single, spectrally filtered, PMT for detection. *The analog output from the PMT is sampled at a rate less than 25 Hz.* Adapting our deep UV lasers to CE instruments is our goal. Our approach is to employ a PMT-based detection system similar to the standard system employed by typical commercial CE instruments using a single PMT or array of PMT's which are gated in synchronism with the laser to provide higher levels of sensitivity and chemical specificity determined by the spectral emission of the native fluorophor emission.

Laser Lifetime

The issue of laser lifetime is of utmost importance in making our deep UV lasers commercially viable. We believe that in order to be commercially viable, the laser needs to operate in field use for over one year without service or other intervention. In order to accomplish this, the mode of operation of the laser needs to be integrated with the application in such a way as to maximize lifetime. We have come to understand that the best model for lifetime of our lasers is based on the number of pulses rather than the number of hours. Our simplest laser (the Series 30) has a hands-off lifetime between 10 and 15 million pulses. The larger and more complex Series 70 laser has a hands-off lifetime between 30 and 50 million pulses. The ultimate lifetime of both laser tubes is about 5x to 10x these lifetimes but optics cleaning is required at the end of each "hands-off" period.

To measure the lifetime in the terms of a typical CE or HPLC detection application, it is important to minimize the number of pulses used to accomplish an electropherogram. The method proposed for sampling is to gate a PMT or array of PMT detectors in synchronism with the laser pulses and collect the native fluorescence emission in each spectral bandpass determined by filters in front of each PMT detector. The output of each PMT is integrated in a storage capacitor and digitized after an integration period typically equivalent to the length of the

laser pulse. The sensitivity of the detection can be selected by selection of the gain of the PMT which is related to PMT voltage, the integration period, and the capacitance of the integration capacitor. If the sensitivity is too high, the integration time can be reduced which will linearly increase the laser lifetime. By sampling the native fluorescence emission in several wavelength regions simultaneously, the chemical identity of the analyte can be determined. In conjunction with the elution time, high levels of specificity can be achieved.

At a sampling rate of 1Hz, the field lifetime of the Series 70 laser is about 20,000 electropherograms assuming an electropherogram took 30 minutes and the laser pulse width was 100 microseconds. Assuming a usage rate of 5 tests per day, 5 days per week, 50 weeks per year, the useful lifetime of the laser in the field will be about 16 years. At a sample rate of 10 Hz the field lifetime will be about 1.6 years. At a sample rate of 25 Hz, the field lifetime will be about 8 months. *If the detection sensitivity is more than needed for the application, the laser pulse width can be reduced with a commensurate improvement in lifetime that is approximately inversely proportional to pulse width.*

The Series 30 laser is much smaller, less expensive and has a lower expected field lifetime. At 1 Hz, the field lifetime of the Series 30 laser is about 6700 electropherograms at a pulse width of 100 microseconds. Again assuming a usage of 5 tests per day, 5 days per week and 50 weeks per year, the useful field lifetime will be about 5.4 years. At a sample rate of 10 Hz it would be about 6 months.

	Series 30	Series 70
Hands-off lifetime	10-15 million pulses	30 – 50 million pulses
Ultimate tube lifetime	500 million pulses	500 million pulses
Hands-off field lifetime in CE	6 years at 1 Hz	16 years at 1 Hz
Hands-off field lifetime in CE	6 months at 10 Hz	1.6 years at 10 Hz

Lifetime Improvement

We are working to improve the fundamental lifetime of the laser tube, which is related to optical contamination. The ultimate lifetime, being over 500 million pulses, is adequate for the CE application at sample rates over 25 Hz, which is equivalent to present commercial CE instruments. However, we cannot give a timeline for these improvements. The lifetimes above represent the current state of our lasers.

One method of improving useful field lifetime in the near term is to vary the sample rate during an elution dependent on the density of peaks. As an example, the first half (or so) of an electropherogram has little if any useful data. Thus, if the laser were operated at a low sample rate during the first 15 minutes of a 30 minute electropherogram, the field lifetime would be effectively doubled. During the second half, the sample rate could be dependent on the rate of change of the information, such that sample rates of 25 Hz or higher would occur during the rise and fall surrounding a peak, but the sample rate would decrease to 1 Hz to 5 Hz between peaks. Another alternative would be to have high sample rates only in the regions of the electropherogram where the data is known to occur. Any of these methods would increase the effective lifetime of the laser.

Background on UV laser induced resonance Raman and resonance fluorescence

High levels of chemical specificity can be obtained using Raman spectroscopy without sample preparation, contact, or destruction⁵. Raman scattering is, in general, a very inefficient process. Normal Raman scatter cross-sections are about 10^{-26} cm² for a major Raman line (1615 cm⁻¹) of a typical microorganism⁶. Normal Raman occurs when the excitation wavelength is far from an electronic absorption band of the material. If the excitation wavelength is within a major electronic absorption band associated with the 1615 cm⁻¹ Raman band, the scattering signal is “resonance” enhanced by as much as eight (8) orders of magnitude, such that the scatter cross-section improves to about 10^{-18} cm². In contrast, maximum resonance (native) fluorescence cross-sections for the same microorganism, measured over a 30nm wide bandwidth near the peak of fluorescence, are about 10^{-11} cm². This is a factor of 10^7 improvement over resonance Raman and clearly demonstrates the sensitivity of resonance fluorescence compared to resonance Raman. However, much higher levels of specificity can be obtained with Raman.

Resonance bands for nucleic and aromatic amino acids occur in the deep UV between about 220nm and 280nm. When excited at wavelengths less than 250nm, Raman scattering occurs within about 20nm to 30nm above the excitation wavelength, corresponding to about 4000 cm⁻¹. Fluorescence occurs only above about 280nm, independent of excitation wavelength. Between the excitation wavelength at about 280nm, there exists a fluorescence-free region in which to observe the weak Raman scattering signal. A Raman shift of 4000 cm⁻¹ corresponds to a wavelength of 247nm when excited at 225nm, 278nm when excited at 250nm and 298nm when excited at 266nm. It is therefore ideal to combine UV resonance fluorescence and resonance Raman spectroscopy to form an integrated tool for both detection and identification of biological agents since they offer a great combination of sensitivity and specificity that do not share overlapping observation wavebands.

Although resonance fluorescence is not the specific subject of this program, it is an integral part of the overall detection method and is closely tied to the excitation wavelengths used for resonance Raman excitation. Therefore we will include a brief discussion of resonance fluorescence here also.

UV Resonance Fluorescence Detection of Biological Agents

All microorganisms require continual input of free energy through cellular metabolism. The source of this energy input is electrochemical potential between electron donors and acceptors. The primary carrier of free energy is adenosine triphosphate (ATP), which is derived from the oxidation of fuel molecules such as carbohydrates and fatty acids. Typical molecules responsible for the transport of energy within cells are porphyrins, quinones, flavins, NADH, etc. Other essential building blocks of living organisms are nucleic acids, amino acids and peptides, sugars and lipids, and polysaccharides. Most of these organic molecules contain chromophores which, when excited at an appropriate wavelength, will provide a signature of the material and give a good indication of the general class to which the microorganism or organic material belongs. Many other organic and inorganic materials also fluoresce that are not harmful to humans.

⁵ Cary, P.R. (1982) *Biological applications of Raman and resonance Raman spectroscopies*, Academic Press, New York.

⁶ Wilfred Nelson, U.Rhode Island, private communications.

However, when the excitation and emission wavebands are carefully chosen, these can be discriminated against with high reliability.

Optimum Fluorescence Excitation and Observation Wavelengths

Resonance fluorescence of biological agents is likely the only technique sufficiently sensitive to discover, *in situ* without any sample preparation, the presence and rough classification of a single or few numbers of microorganisms. It is the only viable method of performing non-contact biological classification of aerosols *in situ*⁷ because of the small dwell time for observation in an aerosol stream.

Fluorescence emission always occurs at wavelengths longer than the excitation wavelength. Fluorescence cross-sections are a function of both the emission and excitation wavelength. If excitation occurs outside of an absorption band, the cross-section will be low, no matter how low the excitation wavelength. It is possible to select an excitation wavelength to emphasize the

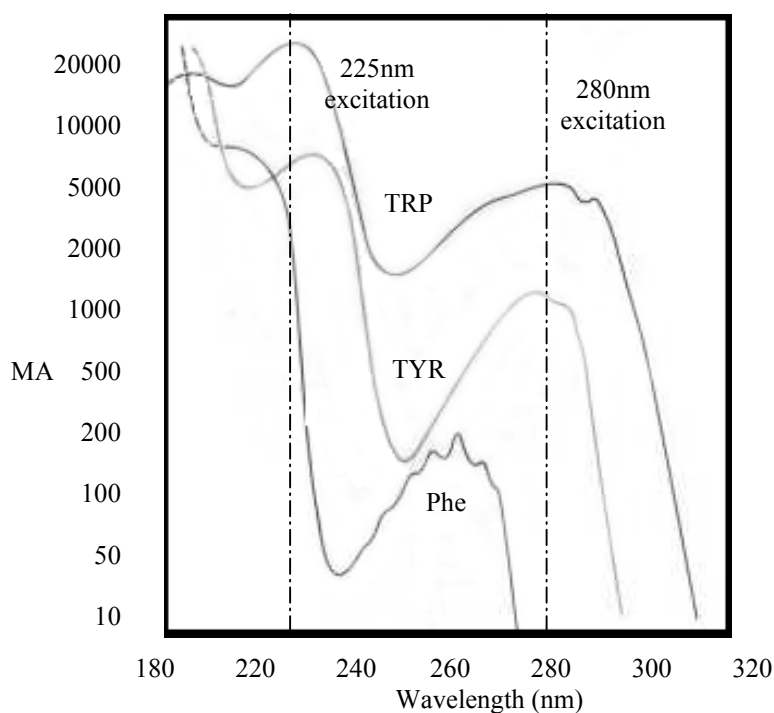


Figure 1. Molar Absorptivity of aromatic amino acids

contrast or targeted biological agents against a wide array of potential background materials. The fluorescence spectrum of a molecule is generally a mirror image of its absorption spectrum and usually forms in broad bands, dependent on the vibrational, rotational and electronic energy level structure of the atom or molecule and its surroundings.

Figure 1 shows the molar absorptivity of the major aromatic amino acids⁸. Note that the molar absorptivity peaks for Trp about 225nm and for Tyr about 230nm. Trp absorption at 225nm is 5 to 10 times stronger than in the traditional excitation wavelength at 280nm. The fluorescence cross-section and related efficiency is similarly higher when excited near their optima. It is a common notion that excitation at shorter wavelengths causes more interference with background materials. This is incorrect as will be shown below. The fluorescence cross-section and subsequent emission intensity is a function of both excitation and emission wavelength. This is illustrated in the following Excitation-Emission-Matrix (EEM) diagrams. EEM diagrams display the fluorescence intensity or cross-section as a function of both excitation and emission wavelength with the iso-

⁷ Faris, G.W., R.A. Copeland, K. Mortelmans, and B.V.Bronk, "Spectrally resolved absolute fluorescence cross sections for bacillus spores", *App.Opt.*, Vol.36, No.4, pp.958-967, 1 February 1997.

⁸ Thomas E. Creighton, **Proteins, Structures and Molecular Properties**, (W.H. Freeman and Company, New York, 1993)

intensity shown as contour lines, as illustrated below in Fig. 2 for *Bacillus subtilis* in both the vegetative and spore form.

It is important to note that both the spores the vegetative cells have two optimum excitation wavelengths, one near 230nm and one near 280nm. Emission maxima vegetative cells at both excitation wavelengths are the same, at about 330nm, as expected. The EEM diagram for *Bacillus subtilis* in spore form (@ 10^4 per ml) is also shown in Fig. 2. Optimum excitation wavelengths are essentially the same for *B. subtilis* spores and vegetative cell. However, the optimum emission wavelength for spores is close to 305nm compared to 340nm for vegetative cells. This is a clearly distinguishable marker feature of spores.

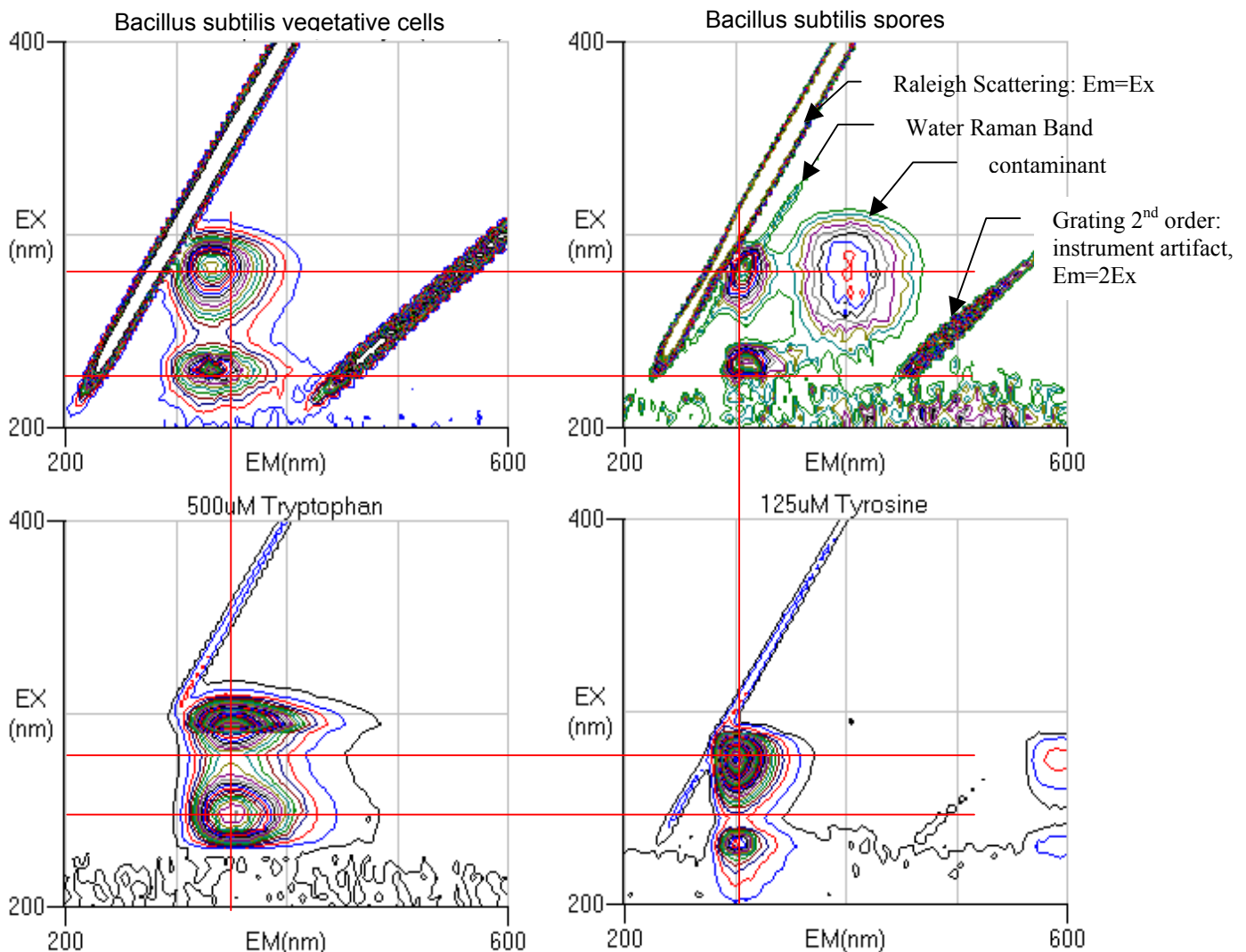


Figure 2. EEM diagrams of *B. subtilis* in spore and vegetative form with Trp and Tyr EEM diagrams

Driks⁹ shows that the spore coat for *B. subtilis* is dominated by tyrosine, whose fluorescence signature peaks near 300nm rather than the tryptophan, whose peak is near 350nm. This is

⁹ Driks, A., "Bacillus subtilis spore coat", Microbiology and Molecular Biology Reviews, Vol.63, No.1, pp.1-20, Mar. 1999.

shown by comparison with the TRP and TYR EEM diagrams shown below the *B. subtilis* in Fig. 2 above. A secondary optima occurring at $Ex=280nm$ and $EM=400nm$ is a result of a denatured alcohol contaminant in the sample. Below in Fig. 3 are the EEM diagrams of several common background materials and minerals. From the above EEM diagrams it is evident that *B.subtilis* vegetative cell fluorescence occurs at shorter wavelengths than pure Trp and long wavelengths than pure Tyr. The spore form is very closely related to Tyr as described by Driks.

The EEM diagrams in Fig. 3, below, illustrate the broad variation of fluorescence fingerprints of many common materials. Most materials exhibit one to three fluorescence peaks. Paper has strong peaks in the blue/green due to doping of paper with fluorescent dyes to enhance “whiteness”. The EEM fingerprints of any of these materials are significantly different from *B. subtilis* in either the spore or vegetative form. However, when detection is accomplished using a

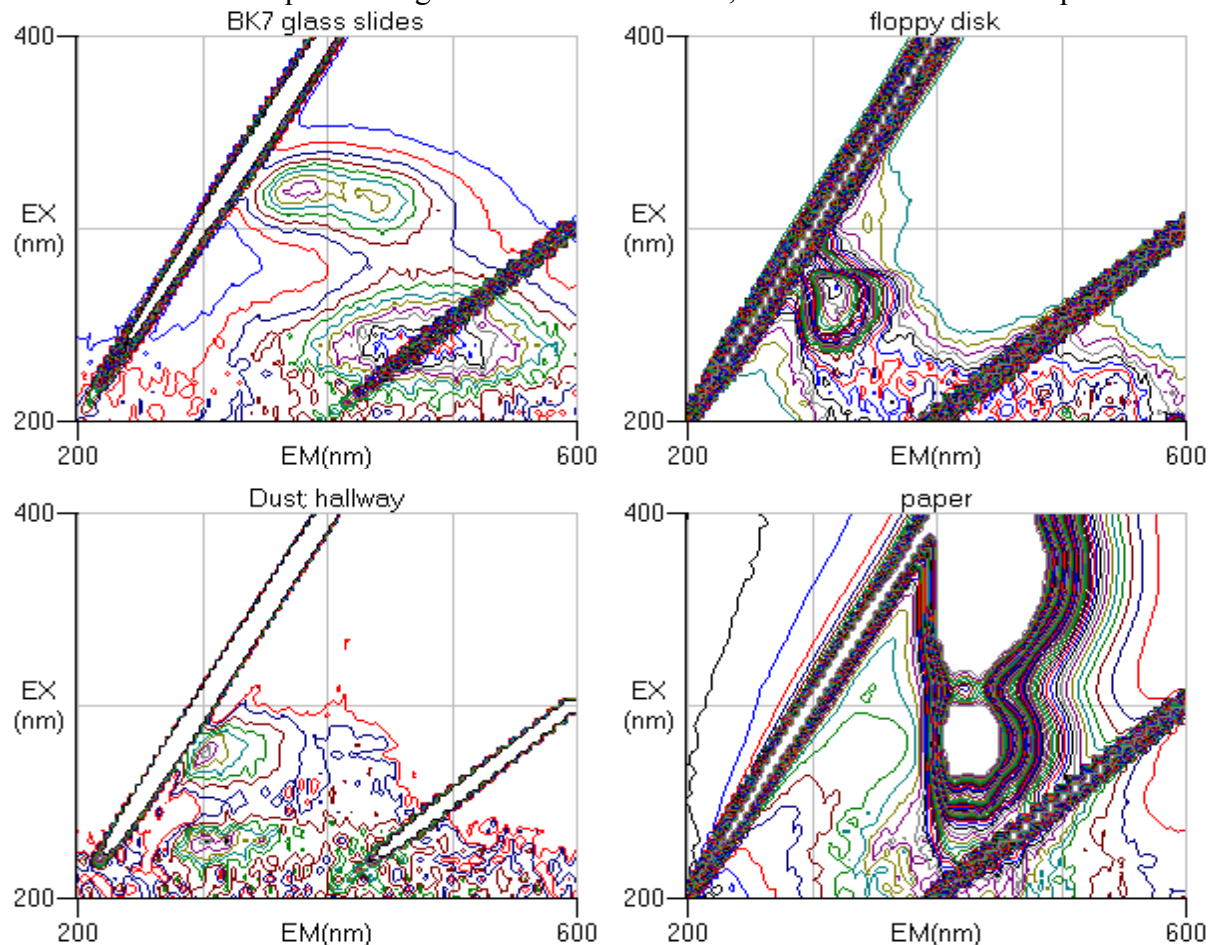


Figure 3. EEM diagrams for sample background materials

single excitation wavelength, some similarities do exist. When excited near 280nm, the emission spectrum of several plastics is similar to *B. subtilis*. However, when excited near 230nm, the spectrum is distinctly different. What is of interest is to select an excitation wavelength and a set of emission observation wavelengths for which biological agents have the highest possible differential fluorescence against the widest range of background materials. It is clear from the above data that deeper UV excitation wavelengths do not “excite everything” as is commonly suggested. Any of several algorithms can be used to optimize the ability to discriminate target

and background materials. It is our best understanding that the false alarm rate can be significantly improved if excitation occurs near 230nm rather than 280nm.

Figure 4 below illustrates the ability to differentiate materials based on their fluorescence signature with only one excitation wavelength at 224nm and a few observation wavebands at 280nm, 325nm, 330nm, 350nm, and 370nm. Each waveband is about 50nm wide. The banded fluorescence emission spectra attained are run through a PCA algorithm to determine where the mineral spectra (open squares) cluster versus where the organics (closed circles) appear. Using tryptophan, which exhibits one of the largest fluorescence cross-sections of the organics, riboflavin, and adenine as organic examples, definitive separation from the minerals (calcite, coal, fluorite, pyrite, and siderite) and rocks (granite and sandstone) is seen. Of note is the separation of the fluorite from the mineral/rock cluster. This is due to fluorite's visible fluorescence emission, which has little effect on the ability to differentiate it from the organics' fluorescence.

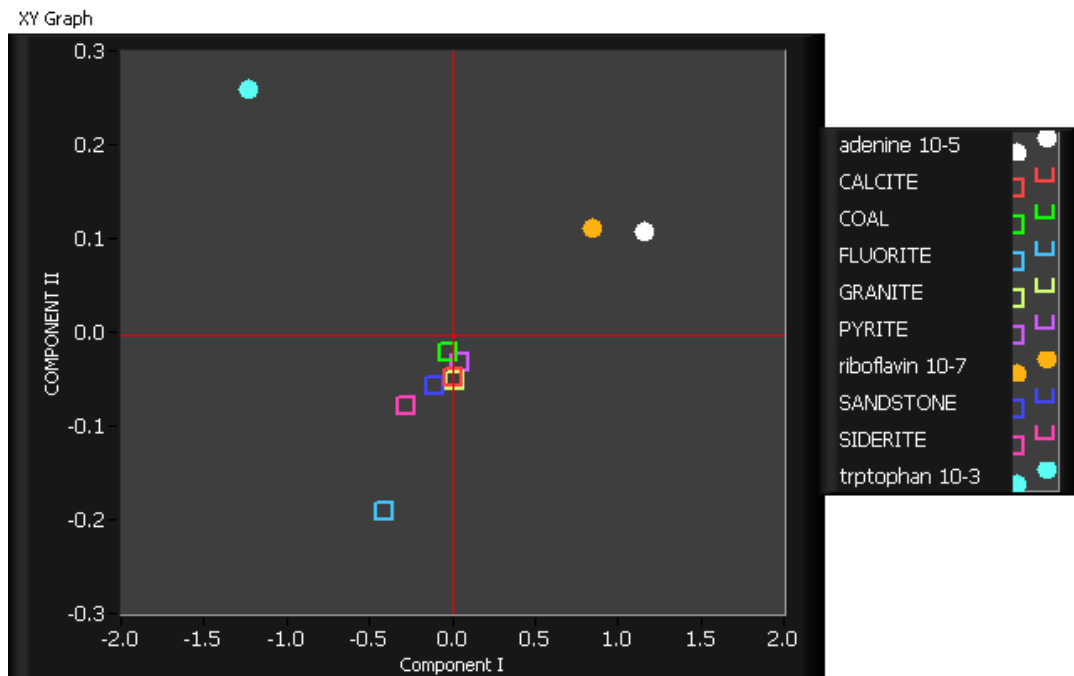
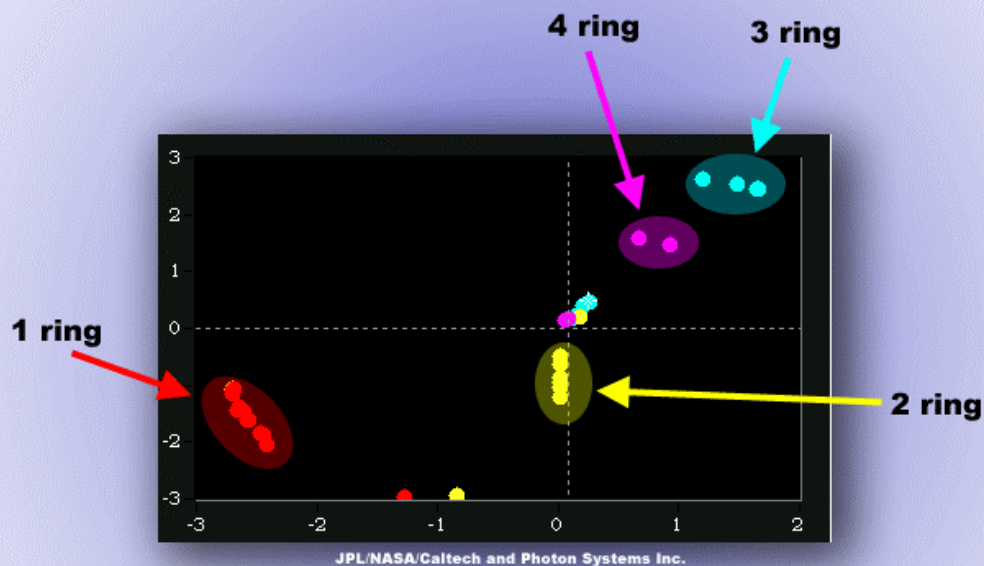


Figure 4. Spectra were acquired on a Hitachi F4500 fluorimeter, excited at 224nm. . (Courtesy R. Bhartia, NASA/JPL)

Another representation of the ability to distinguish chemicals using only a few fluorescence detection bands is shown below in Fig. 5. Rather than the PCA representation shown above, Fig. 5 uses a band differencing scheme to distinguish between chemicals with varying numbers of fused and unfused benzene ring structures. Within each group the variance of fluorescence signature can identify differences in side groups. Aromatic amino acids can be clearly distinguished using fluorescence in a few numbers of bands.

PAH Fluorescence: Separation using bandpass filters



43 PAH's: Fluorescence emission with 6 computer simulated bandpass filters. (ex 250-267nm)

**Variance within Groups due to functional groups (-methyl, -dimethyl etc.)
Outliers are additions of conjugated bonds (C=C) or non aromatic rings**

Figure 5. Illustration of ability to distinguish broad ranges of hydrocarbon materials. Data from Hitachi F4500. Courtesy of R. Bhartia, JPL/NASA/Caltech.

UV Resonance Raman Identification of Biological Agents

Over the past ten years UV resonance Raman spectroscopy has been increasingly used for detection and identification of microorganisms and study of cellular function¹⁰¹¹¹²¹³¹⁴. UV resonance Raman spectroscopy allow the measurement of clear band structures within the electronic absorption manifold of the target biological molecules and thereby enables the ability to more clearly characterize unknown biological materials. Photon Systems has benefited from close collaborations and association with Professors Sanford Asher of the University of Pittsburgh and Wilfred Nelson of the University of Rhode Island in conjunction with our

¹⁰W.H.Nelson, R. Manoharan and J.F. Sperry, "UV Resonance Raman Studies of Bacteria", App. Spect. Reviews, 27 (1), pp67-124, 1992

¹¹ S. Chadha, W. H. Nelson and J.F. Sperry, "Ultraviolet micro-Raman spectrograph for the detection of small numbers of bacterial cells", Rev. Sci. Instrum. 64 (11), pp.3088-3093, Nov. 1993

¹² Z. Chi and S. A. Asher, "UV resonance Raman Determination of Protein Acid Denaturation", Biochemistry, 37, pp.2865-2872, 1998.

¹³ N.Cho and S.A. Asher, "UV resonance Raman studies of DNA-Pyrene interactions", J.Am. Chem.Soc. 115, pp.6349-6356, 1993

¹⁴ F. Sureau, et.al., "An ultraviolet micro-Raman spectrometer: Resonance Raman spectroscopy within a single cell", App.Spect., 44, No.6, pp.1047-1051, 1990

development of deep UV lasers and miniature Raman instruments. Both of these men are known for their groundbreaking work in UV resonance Raman spectroscopy, especially as it applies to characterization of organic molecules and the molecules of life. We recently published a paper with Prof. Asher¹⁵ and have participated in NASA-sponsored research with Prof. Nelson.

It has been clear for several years that unique ultraviolet resonance Raman spectral signatures can reliably be detected in as few as 20 bacterial cells with low power consumption and low photon flux levels (Nelson, 1993¹⁶; Nelson, et.al¹⁷, 1993; Chadha, et.al., 1993¹⁸). In fact, UVRR has made possible the detection and characterization of single cells.

Taxonomic Raman Marker Bands

A summary of the major taxonomic marker bands of highly degenerate functional groups occurring within microorganisms is shown below in Table I.

Table I. Major Taxonomic Raman marker bands for biological agents

Material	Raman Band Locations					
Tryptophan	753	879	1011	1353	1555	1615
Tyrosine	831	852	1180	1210		1615
Guanine				1320 1365	1485	1577 1603
Adenine				1337	1485	1580
Cytosine					1530	
Dipicolinic Acid			1017	1195	1396	1446

Identification of biopolymers or organisms using UV Raman spectroscopy depends on the ability to produce interpretable, reproducible spectra. DNA and cell surface antigens are the most attractive targets as potential markers for cellular or bacterial identification. Identification of organisms using UV Raman spectroscopy has focused on the ratio of a few taxonomic marker bands (Ref.17). These band markers are based on ratios of tryptophan and tyrosine and DNA base pairs that can be characteristic of an organism. As mentioned previously, most biological materials have repeating functional groups that are highly degenerate. These include nucleic acid base pairs and aromatic amino acids. These repeating units have Raman spectra that are very similar to the spectra of the monomers upon which they are based. Raman spectra of *B. cereus* in several forms is shown below in Fig. 5 in using 242nm excitation: vegetative, spore and germinated spore (Ref.17). Major Raman marker bands are shown at 1019 cm⁻¹, 1485 cm⁻¹, 1530 cm⁻¹, 1555 cm⁻¹, and 1615 cm⁻¹. The measurement bandwidth illustrated is about 25 cm⁻¹.

¹⁵ Sparrow, M.C., J.F. Jackovitz, C.H. Munro, W.F. Hug, and S.A. Asher, "A New 224nm Hollow Cathode UV Laser Raman Spectrometer", *J. App. Spectroscopy*, Vol. 55, No. 1, Jan 2001.

¹⁶ Nelson, W.H. (1993) *Rev Sci. Inst.* (11):3088-3093

¹⁷ Nelson, W.H., Manoharan, R., and Sperry, J.F. (1992) *Appl. Spect. Rev.* 27(1), 67

¹⁸ Chadha, S., Nelson, W.H., Sperry, J.F. (1993) *Rev. Sci. Inst.* (11):3088-3093

Bacteria can be characterized as Gram positive versus Gram negative based on the $1555\text{ cm}^{-1}/1615\text{ cm}^{-1}$ intensity ratio.

Gram negative bacteria have a much higher ratio of the tryptophan intensity at 1011 cm^{-1} or 1555 cm^{-1} compared to the Tyr + Trp intensity at 1615 cm^{-1} . In general, this ratio is described as the intensity in broad spectral regions centered near the 1555 cm^{-1} and 1615 cm^{-1} Raman bands. However, the exact position, center of gravity, band width, and other features of each band can provide more detailed identification of bacteria. However, the relationships are presently unknown. It is believed that these marker bands primarily describe the surface composition of an organism.

Within Gram positive organisms such as spores, or vegetative cells there is further sub-classification G+C percentage. This is determined by the $1530\text{ cm}^{-1}/1485\text{ cm}^{-1}$ Raman band intensity ratio.

The intensity of the 1485 cm^{-1} peak is taken as closely proportional to the total amount of nucleic acid on a molar basis (DNA + RNA) in the cell. The intensity of the peak at 1530 cm^{-1} can be assumed to be proportional to the moles of cytosine in the nucleic acids. It follows that the mole fraction of G+C in the bacteria should be proportional to the ratio of the 1530 cm^{-1} and 1485 cm^{-1} peaks.

Following is a graph of the $1530/1485\text{ cm}^{-1}$ ratio versus the known percentage of G+C of DNA in 14 different bacterial species grown on TSA and in TSB, respectively (Ref.17). The peak intensity ratios versus molar percent G+C are linear dependent, as shown in Fig. 6.

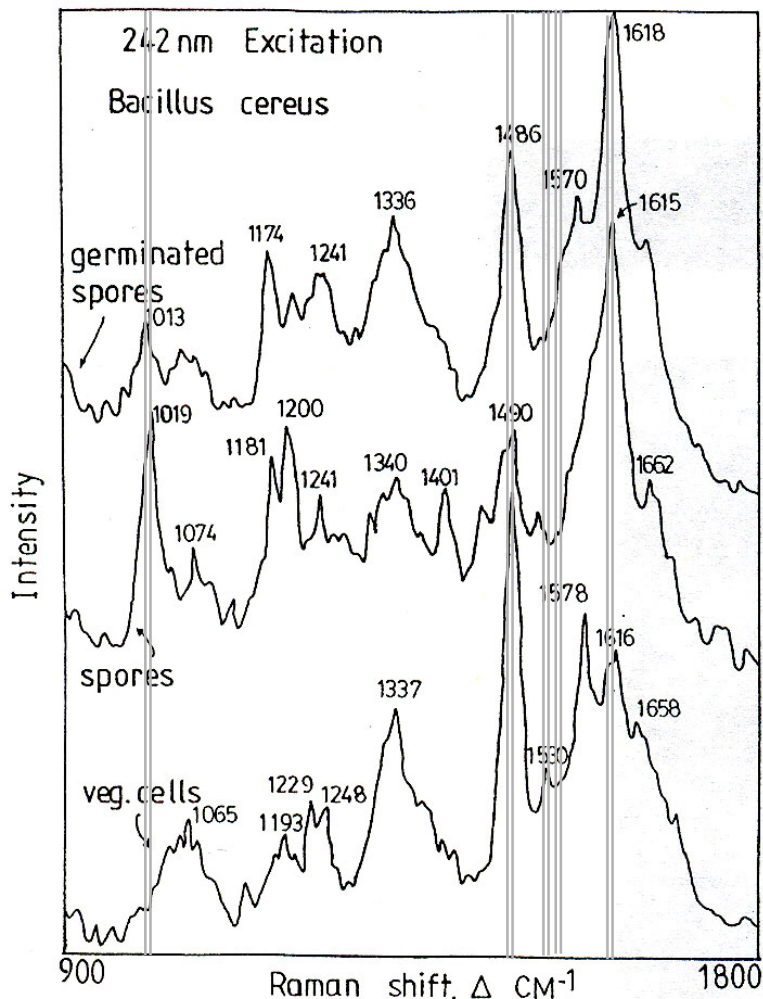


Figure 5. Resonance Raman spectra of *B. cereus* in various forms(Ref.10)

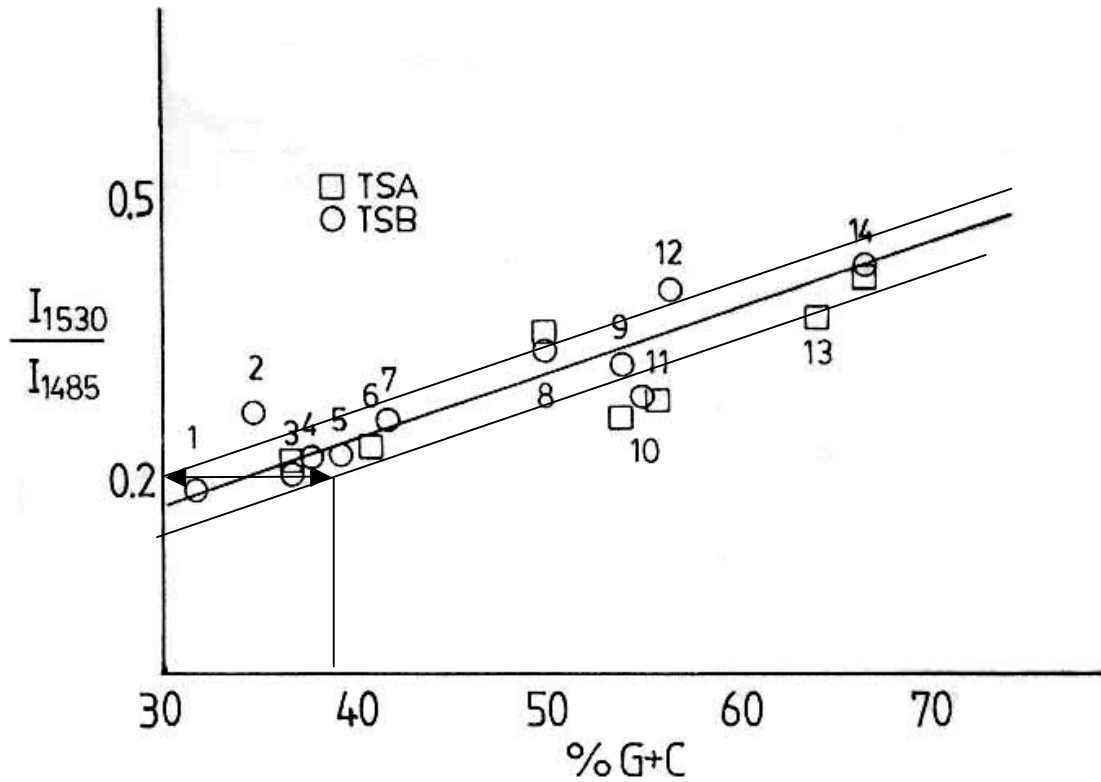


Figure 6. Plot of $1530\text{ cm}^{-1}/1485\text{ cm}^{-1}$ versus known G+C for 14 bacterial species. 242nm excitation. (Adapted from Ref.10)

Three lines are shown in Fig. 6 which represent the mean and \pm one standard deviation of the data. This preliminary estimate illustrates the potential to identify an organism within about ± 3 to ± 5 mole percent G+C. In combination with identification of the Gram polarity and whether the organism is a spore, the G+C content can provide significant specificity in identification of biological agents. The organisms employed in Fig. 6 are tabulated below in Table II.

Table II. DNA mole fraction for Guanine + Cytosine for bacteria in Fig. 6

Plot No.	Organism	Mole% G+C	Gram	Spores	Virulence class ^g
	Clostridium botulinum	28.2 ⁱ	+	X	2
	Rickettsia prowasecki	28.9 ⁱ	-		3
	Staphylococcus aureus	32.8 ^b	+		2
1	Bacillus cereus	32 ^a	+	X	1
2	Enterococcus faecalis	34-36 ^a 37.5 ^b	-		1
	Staphylococcus simulans	34-38 ^a	+		1
	Bacillus anthracis Ames	35.2 ^b	+	X	2
	Streptococcus agalactiae	35.5 ^b	+		1
4	Proteus vulgaris	36-40 ^a	-		1
3	Bacillus magaterium	37 ^a	+	X	1
5	Proteus mirabilis	39.5 ^a	-		1
6	Bacillus subtilis	41 ^a	+	X	1
7	Acinetobacter calcoaceticus	42 ^a	-		2
	Bacillus subtilis	43.5 ^b	+	X	1
	Shewanella oneidensis MR1	45.9 ^b	-		1
	Yersinia pestis.	47.6 ⁱ	-		3
	Vibrio cholerae	47.6 ⁱ	-		3
8	Escherichia coli, K12-MG1655	50.7 ^b	-		2
	Shigella dysenteriae	50 ⁱ	-		2
	Samonella tphi	52.1 ⁱ	-		2
9	Enterobacter aerogenes	54.3 ^a	-		1
10	Alcaligenes faecalis	54.8 ^a	-		1
11	Enterobacter cloacae	55.4 ^a 57.2 ^b	-		1
12	Aeromonas hydrophila	55.7 ^a	-		1
	Brucella suis 1330	57.2 ^b	-		3
	Brucella melitensis	57.2 ^c	-		3
	Aeromonas hydrophila	59-62 ^c	-		1
	Pseudomonas putida	61.4	-		1
13	Pseudomonas aeruginosa	64 ^a , 66.4 ^b	-		1
14	Micrococcus luteus	66.3 ^a	+		1
	Alcaligenes faecalis	66.7-69.9 ^c	-		1
	Burkholderia pseudomallei	68.06 ⁱ	-		3

a=A.I.Laskin & H.A.Lechvallier(eds), CRC Handbook of Microbiology, Vol.II, CRS Press, Cleveland, 1973. b=tigr, i=Sanger Inst.

Biological Agent Identification Specificity

One possible detection and identification strategy for biological agents using laser induced resonance fluorescence and UV Raman spectroscopy is as follows:

- a. Determine if a particle is biological or non-biological based on laser induced resonance fluorescence measured in the 300nm region.
- b. If particle is biological, measure the relative UV Raman intensity at five (5) Raman bands centered at 1017 cm^{-1} , 1485 cm^{-1} , 1530 cm^{-1} , 1555 cm^{-1} and 1615 cm^{-1} .
- c. Determine if the particle is Gram positive or negative based $1555\text{ cm}^{-1}/1615\text{ cm}^{-1}$ ratio.
- d. Determine if the particle is a spore based on the $1017\text{ cm}^{-1}/1615\text{ cm}^{-1}$ ratio.
- e. Determine the GC% based on the $1530\text{ cm}^{-1}/1485\text{ cm}^{-1}$ ratio.

Measurement of the Raman scattering in only five (5) broad ($\approx 40\text{cm}^{-1}$) bands ***provides knowledge of the: Gram polarity; form of organism; and G+C percent.*** These measurements can be made rapidly and correlated using any of several artificial neural net or PCA/PCO algorithms to give a relatively high degree of confidence in identifying organisms within a narrow range. These measurements could be made in sub-second time scales and possibly as short as a millisecond or faster.

Using this fast and simple 5-band Raman technique, it would appear that it is unlikely this method would be able to specifically differentiate *B. anthracis* against a background containing a wide range of other similar spore interferants since the detection accuracy corresponds to only about $\pm 4\%$ in G+C concentration. The closest spore to *B. anthracis* at GC=35.2% is *B. cereus* at 32% ($\Delta=3.2\%$) and *B. magisterium* at 37% ($\Delta=1.8\%$). All three are spore formers and all are Gram positive. So none of the discriminators would have differentiated between these organisms with a low false alarm rate. However, this fast method will probably enable discrimination of *B. subtilis* from *B. anthracis*. In addition, this method would be able to discriminate anthrax from a wide range of other bacterial spores and other microorganisms and identify them within a small range.

There are many UV Raman spectroscopic options that have yet to be evaluated to reduce the false alarm rate in identifying *B. anthracis* or other virulent microorganisms. The fast and simple approach described above does not take advantage of the much larger wealth of information contained in UV Raman spectra. Substantial differences in taxonomic marker band intensity, peak position, center of gravity, and band shape occur for each of the basic Raman marker bands. These are a result of environmental and conformational differences between organisms as well as more subtle compositional differences. In addition, there are other Raman marker bands that are clearly measurable which may give further discrimination to microorganism identification. In order to provide a higher level of biological agent specificity, higher resolution Raman spectra would be required. A reasonable way to triage a target would be to follow the laser induced resonance fluorescence and broadband UV resonance Raman with high resolution UV resonance Raman. Each of these techniques is successively more time consuming, less sensitive and more specific. At present there is no clear model to provide higher specificity based on more subtle nuances of the Raman spectra such as peak position or center of gravity variations due to difference in microorganisms.